

PEAKD – UgeA, UgmA AFM

1

1 **Quantifying the importance of galactofuranose in *Aspergillus nidulans* hyphal wall**
2 **surface organization by atomic force microscopy.**

3

4 **Running Title: The role of Galf in *A. nidulans* wall organization**

5

6 Biplab C. Paul^{a,d}, Amira M. El-Ganiny^{b,c,d}, Mariam Abbas^a, Susan G. W. Kaminsky^{b,e}, Tanya
7 E. S. Dahms^{*a,e}

8

9 ^a Department of Chemistry and Biochemistry, University of Regina, 6262 Wascana Parkway,
10 Regina SK S2S 0A2, Canada.

11 ^b Department of Biology, University of Saskatchewan, 112 Science Place, Saskatoon SK S7N
12 5E2, Canada.

13 ^c Microbiology Department, Faculty of Pharmacy, Zagazig University, Egypt.

14 ^d Contributed equally to the research.

15 ^e Contributed equally to the writing.

16 * Author to whom correspondence should be addressed. Email: tanya.dahms@uregina.ca;

17 Telephone: 1 306 585 4246

18 **Abstract**

19 The fungal wall mediates cell-environment interactions. Galactofuranose (Gal_f), the five-
20 member ring form of galactose, has a relatively low abundance in *Aspergillus* walls yet is
21 important for fungal growth and fitness. *A. nidulans* strains deleted for Gal_f biosynthesis
22 enzymes UgeA (UDP-glucose-4-epimerase) and UgmA (UDP-galactopyranose mutase) lacked
23 immunolocalizable Gal_f, had growth and sporulation defects, and had abnormal wall
24 architecture. We used atomic force microscopy and force spectroscopy to image and quantify
25 cell wall viscoelasticity and surface adhesion of *ugeA*Δ and *ugmA*Δ strains. We compared
26 them with a wild type (AAE1) and the *ugeB* deletion strain, which has wild type growth and
27 sporulation. Our results suggest that UgeA and UgmA are important for cell wall surface
28 subunit organization and wall viscoelasticity. The *ugeA*Δ and *ugmA*Δ strains had significantly
29 larger surface subunits and lower cell wall viscoelastic moduli than those of AAE1 or *ugeB*Δ
30 hyphae. Double deletion strains, [*ugeA*Δ, *ugeB*Δ] and [*ugeA*Δ, *ugmA*Δ], had more disorganized
31 surface subunits than single deletion strains, and changes in wall surface structure correlated
32 with changes in its viscoelastic modulus for both fixed and living hyphae. Wild type walls had
33 the largest viscoelastic modulus, while those of the double deletion strains had the least. The
34 *ugmA*Δ and particularly the [*ugeA*Δ, *ugmA*Δ] strains were more adhesive to hydrophilic
35 surfaces than wild type, consistent with changes in wall viscoelasticity and surface
36 organization. We propose that Gal_f is necessary for full maturation of *A. nidulans* walls during
37 hyphal extension.

38 **Introduction**

39 The fungal wall supports and shields the hyphal cytoplasm, and mediates interactions
40 between the cell and its environment. Fungal walls are typically about 30 % of cell dry weight
41 (7, 10), and a similar portion of the fungal genome is thought to contribute to cell wall
42 biosynthesis and/or maintenance (11, 17). Fungal walls are composed of a variety of
43 carbohydrate polymers (7, 11, 15), however, deleting many wall biosynthesis genes appears to
44 be compensated by genetic redundancy and/or by induction of the cell wall integrity pathway
45 (6, 7, 23).

46 The *Aspergillus* wall is reinforced by chitin fibrils, and has a matrix containing alpha- and
47 beta-glucans, other sugars including galactomannans, and proteins. Galactofuranose (*Galf*) is
48 the five-member ring form of galactose that is found in the cell walls of *Aspergillus* (6, 7, 23),
49 other fungi (reviewed in (15)), and certain other microbes (3). Deletion of
50 UDP-galactopyranose mutase in several *Aspergillus* species has shown that *Galf*, despite its
51 relatively low abundance, is important for wild type fungal growth, cell morphogenesis, hyphal
52 adhesion, wall architecture, and spore development (6, 8, 9, 14, 16, 25) and may mediate
53 pathogenesis (1, 21-23).

54 The *A. nidulans* gene products UgeA (UDP-glucose-4-epimerase) (8), and UgmA (UDP-
55 galactopyranose mutase) (9) catalyze sequential steps in *Galf* biosynthesis (Figure 1). The
56 *ugeA* Δ and *ugmA* Δ deletion strains have similarly compact colonies, aberrant hyphal growth
57 and reduced sporulation. The hyphal walls of these strains differ from wild type and with each
58 other as visualized using transmission electron microscopy (TEM) (8).

59 Atomic force microscopy (AFM) imaging uses a fine-tipped probe mounted on a flexible
60 cantilever to raster scan the surface of an object generating a topographic map. An
61 approach-retract cycle of the AFM probe, called force spectroscopy (FS), can be used to
62 calculate the viscoelastic modulus of the whole organism or its cell surface, and surface

63 adhesion. Previously we used AFM to show that *A. nidulans* cell walls of growing hyphal tips
64 differ from those of mature regions (18), and to document changes associated with spore
65 [swelling](#), germination and the non-polarized hyphal growth of temperature sensitive mutants
66 (19). Here, we compare the hyphal walls of wild type and a suite of *Galf* biosynthesis pathway
67 deletion strains using TEM, AFM and FS to gain a better understanding of the role played by
68 *Galf* in *Aspergillus nidulans* cell wall organization.

69

70 **Materials and Methods**

71

72 **Strains and culture conditions**

73 *Aspergillus nidulans* and *Escherichia coli* strains were grown as described in (8, 9)
74 using media formulated as described in (13). Deletion strain construction followed procedures
75 described in (8, 9) using *nkuA* Δ strains, plasmids and primers listed in supplemental [Table SA](#).
76 AN2951 (*ugeB*) was deleted from A1149 using *AfpyroA* as selectable marker (amplified from
77 pTN1) to generate [AAE9](#). Thereafter, *ugeA* was deleted from [AAE9](#) using *AfpyrG* as selectable
78 marker (amplified from pAO18) to create the [*ugeA* Δ , *ugeB* Δ] double deletion strain [AAE10](#).
79 Construction of [AAE8](#) [*ugeA* Δ , *ugmA* Δ] was described in (8).

80

81 **Confocal fluorescence and transmission electron microscopy (TEM).**

82 Samples were prepared for light microscopy as described in (9). [Briefly, freshly](#)
83 [harvested spores were grown on coverslips for 16 h at 28 °C in complete medium \(CM\) liquid,](#)
84 [fixed and stained with Hoechst 33258 \(for nuclei\) Calcofluor \(for cell walls\), then imaged by](#)
85 [confocal microscopy. Hyphal width and basal cell length were measured at septal positions in](#)
86 [mature regions \(~ 40 \$\mu\$ m from the tip\) for 50 cells per strain using LSM examiner.](#)

87 For TEM, wild type and gene deletion strains were grown on dialysis tubing laid over
88 complete medium agar for 1 d at 28 °C, then fixed, embedded, and sectioned for as described
89 previously (9). Hyphal wall thickness was measured on TEM cross-sections of ten hyphae per
90 strain, typically three measurements per hypha, at places where the cell membrane was crisply
91 focussed.

92

93 **Atomic force microscopy.**

94 Samples for imaging fixed hyphae were prepared for AFM as previously described (18,
95 19). Briefly, conidia were germinated in liquid growth medium between two glass coverslips for
96 16 h. The top coverslip was carefully removed, and the hyphae were fixed with 3.7 %
97 formaldehyde in 50 mM phosphate buffer, pH7.0, containing 0.2 % Triton X-100, followed by
98 rinsing with distilled water and air drying. For live cell AFM imaging, hyphae were grown on
99 dialysis tubing (Spectrapor, 12-14 kDa) overlaying agar medium. After 16 h growth, the dialysis
100 tubing was transferred to a glass coverslip. Sterile Whatman #4 filter paper placed beneath the
101 dialysis tubing was used to deliver liquid growth medium by capillary action, ~ 20 µL at a time.

102 An Explorer™ AF microscope (Veeco <http://www.veeco.com/>) with a dry scanner
103 (Veeco, model 5460-00) was used for contact mode imaging and force spectroscopy (FS), as
104 previously described (18, 19). Hyphae were visualized by CCD camera (200 ×) and imaged
105 first at low resolution (200 × 200 lines per scan). All topographic and lateral force data were
106 collected from high-resolution images (500 × 500 lines per scan) of fixed and live (scan rate =
107 1 and 2 Hz, respectively) cells using Si₃N₄ probe tips (Veeco model #1520-00, k = 0.05 nN/nm,
108 nominal resonance n = 17 kHz). Images represent typical results. AFM tip size and shape was
109 calibrated using gold spheres according to (27).

110

Force spectroscopy

Cantilever spring constants, k_c , were determined prior to each force measurement using resonance frequencies according to (5). Tip-sample interaction was tracked by cantilever deflection as a function of Z piezo elongation during probe approach and retraction. For soft materials, meaningful FS comparisons often depend on the velocity of the surface approach (4). In this case, the approach velocity did not significantly affect the hyphal spring constant (data not shown), but this parameter was kept constant (100 nm/s) to facilitate comparison of viscoelastic moduli between samples. Repeated measurements of individual sites on mature walls gave consistent values, and images obtained before and after FS were unchanged (data not shown), indicating that the walls were not damaged during data collection. Values were averaged from force curves collected in triplicate at ten separate points on the surface of mature hyphal walls ($\geq 40 \mu\text{m}$ from the tip) for five hyphae per sample and typically three different samples.

Force approach curves measure the unit force (nN) required to indent a surface a given distance (nm), so the slope corresponding to the b-c segment of the approach cycle (refer to Figure 5A) was used to examine the relative cell wall elasticity. FS data were plotted as deflection (nA) versus distance (nm), converted to force (nN) versus distance (nm) curves using the piezo sensor response, and the slope of the line b-c (m) in nN/m used to determine the spring constant k_w of the cell wall according to:

130

$$k_w = m_s k_c / m_h - m_s \quad (1)$$

132

133 where m_s is the sample slope and m_h is the slope for a hard surface (mica). The value of k_w
134 was used for the subsequent determination of Young's modulus according to the equation
135 (28):

$$137 \quad E \sim 0.80 k_w/h (R/h)^{1.5} \quad (2)$$

138
139 where E is the cell wall viscoelastic (Young's) modulus, R is the hyphal radius measured by
140 either TEM or AFM, and h is the thickness of the cell wall measured by TEM. Surface adhesion
141 values were measured from the last segment of the retraction cycle (Figure 5A, segment e–f).
142 If there is a chemical attraction between the sample and the Si_3N_4 AFM probe, which is
143 hydrophilic, segment e–f will be a measure of its intensity in nN.

144

145 **Data Processing and Analysis**

146 AFM images were processed using horizontal levelling, with the maximal height
147 adjusted for optimum contrast (SPMLab version 6.0 software, Veeco). [Hyphal widths at mature](#)
148 [regions \(~ 40 \$\mu\text{m}\$ from the tip\) and](#) surface feature dimensions from topography and lateral
149 force images were measured at the FWHM of the peak height. AFM data are presented as
150 mean \pm standard deviation or as ranges of values. TEM and confocal data are presented as
151 mean \pm standard error of the mean. Differences in the mean subunit sizes of wild type and
152 deletion strain hyphae were tested by a one-way ANOVA (InStat 3, GraphPad Prism).
153 Standard errors propagated through equations 1 and 2 were calculated for viscoelastic moduli,
154 and a Student's t -test (two-tailed) was used to assess significant difference between values
155 (InStat3, GraphPad Prism).

156

157 **Results**

158 Building on our previous experience using AFM to study *A. nidulans* hyphae (18, 19) we
159 compared a suite of *A. nidulans* strains deleted for GalF biosynthesis enzymes UgeA and
160 UgmA, the near-isogenic wild type strain AAE1, a strain deleted for an epimerase (UgeB) that
161 did not affect hyphal morphogenesis, and double deletion strains [*ugeA*Δ, *ugeB*Δ] and [*ugeA*Δ,
162 *ugmA*Δ]. Double mutants were used to further explore the function of individual gene products.
163 Even enzymes that mediate a known biochemical function may have collateral defects in a
164 deletion strain based on protein-protein interactions, for example if the protein is part of a
165 scaffold for a multi-enzyme.

166

167 **Characterization of *Aspergillus nidulans ugeB***

168 *Aspergillus nidulans* ANID2951.4 (which we named UgeB) shares 38 % amino acid
169 sequence identity with UgeA (8), and had been annotated as a UDP-glucose/galactose-4-
170 epimerase (www.broadinstitute.org/annotation/genome/aspergillus_group/). The *ugeB*
171 genomic sequence has a single exon that encodes a 428 amino acid peptide. The *ugeB* cDNA
172 could not be amplified (three attempts), unlike *ugmA* (7) and *ugeA* (8). We deleted *ugeB*
173 (Figure SA) as described in (9), and confirmed the deletion using PCR (Table SA, Figure SA).
174 A [*ugeA*Δ, *ugeB*Δ] strain was generated and confirmed (Figure SB) as described in (8). The
175 *ugmA*Δ strain was described in (9) and the *ugeA*Δ and [*ugeA*Δ, *ugmA*Δ] strains were
176 described in (8). UgeB was expressed *in vitro* using the genomic sequence, which does not
177 contain introns, purified, and shown to convert UDP-galactose into a product that is not
178 UDP-glucose, following the procedure shown in (8, and data not shown). This unknown
179 product awaits conclusive identification.

180 The *ugeB* sequence was put under the control of the *AlcA* promoter and also tagged
181 with red fluorescent protein (El-Ganiny and Kaminskyj, in preparation), then over-expressed by

182 culturing on CM containing 100 mM threonine (CMT). Under these conditions, *pAlcA-ugeB-rfp*
183 was expressed, albeit weakly, in conidia and to a lesser extent in mature hyphae (Figure SC),
184 but was not detectable in hyphal tips (data not shown).

185 **Morphology of *Aspergillus nidulans* strains deleted for *Galf* biosynthesis genes**

186 Confocal microscopy images showing the hyphal morphology of the suite of *Galf*
187 biosynthesis deletion strains examined in this study (AAE1, *ugeA* Δ , *ugeB* Δ , [*ugeA* Δ , *ugeB* Δ],
188 *ugmA* Δ , [*ugeA* Δ , *ugmA* Δ]) are shown in Figure 2. Strain morphometry is described in Table 1.
189 Unlike the previously described *ugeA* Δ and *ugmA* Δ deletion strains, which had wide and highly
190 branched hyphae and reduced sporulation (8, 9), the *ugeB* Δ strain had wild type morphology
191 hyphae and growth rate, and abundant sporulation (Table 1; Figure 2; data not shown). The
192 [*ugeA* Δ , *ugeB* Δ] strain was viable when grown on media containing glucose as carbon source,
193 but it did not form colonies on media containing galactose as the sole carbon source (due to
194 *ugeA* Δ), and its hyphae were wide and branched like those of *ugeA* Δ (Table 1; Figure 2).

195 Transmission electron micrographs of hyphal cross-sections showed that the walls of
196 *ugeA* Δ and *ugmA* Δ strains were two-fold and four-fold thicker, respectively, than those of AAE1
197 (Table 1, Figure 3) (8, 9). Given the general correlation between hyphal morphology and wall
198 thickness (e.g. 8, 9, 11, 12, 20, 24), we expected that the hyphal wall thickness of *ugeB* Δ might
199 be similar to AAE1. Instead, the *ugeB* Δ strain hyphal walls were almost two-fold thicker than
200 AAE1 (Table 1, Figure 3). Also unexpectedly, the [*ugeA* Δ , *ugeB* Δ] strain hyphal walls were
201 about twice as thick as either single deletion strain, even thicker than those of the [*ugeA* Δ ,
202 *ugmA* Δ] strain (Table 1, Figure 3).

203 TEM images of the *ugeA* Δ (Supplementary Figure Cb in 8) and *ugeB* Δ (data not shown)
204 strains grown in liquid shake culture accumulated debris, not observed for the same strains
205 grown on dialysis tubing (Figure 3) or for the [*ugeA* Δ , *ugeB* Δ] strain (data not shown).

206

207 Atomic force microscopy imaging of wild type and Galf gene deletion strains.

208 We used AFM imaging to acquire high-spatial resolution information about the hyphal
209 wall surfaces of two wild type and four Galf biosynthesis gene deletion strains. AFM imaging
210 provides quantitative depth resolution, thus facilitating surface subunit measurements (18, 19).
211 Our previous work demonstrated that for the wild type strain, A28, the walls of hyphal tips and
212 tips of lateral branches had matured by 3 μm behind the apex, at which point their surfaces
213 resembled unbranched regions 20 μm and 40 μm behind the tip (18). To ensure that wall
214 surfaces were mature for all strains, we chose analysis sites that were at least 40 μm behind
215 the hyphal tips, expecting that wall maturation might be slower in the Galf biosynthesis gene
216 deletion strains. AFM data can be collected from living or fixed cells (e.g. (18)). We present
217 images of fixed hyphae for comparing wall surfaces amongst the suite of Galf biosynthesis
218 gene deletion strains, since hyphal wall subunit size and distribution were similar to living cells
219 but were more clearly defined (18).

220 Contact mode AFM imaging simultaneously collects topography and lateral force
221 information. The latter represents a convolution of topography and tip-sample interactions for
222 rough samples, thus producing relief images with more clearly defined edge features (18).
223 High resolution images of fixed wild type (AAE1) and Galf biosynthesis gene deletion strain
224 hyphae (Figure 4) show distinct differences in their surface subunit size (Table 1) and packing.
225 AAE1 hyphae had small rounded subunits with a consistent size and even packing. In contrast,
226 both the *ugeA* Δ and *ugmA* Δ strain hyphae had substantially larger and more variable-sized
227 hyphal wall surface subunits than AAE1, and also had more disorganized subunit packing. The
228 [hyphal wall of the *ugeB* \$\Delta\$ strain most closely resembled](#) that of AAE1, but with slightly
229 elongated subunits. The [*ugeA* Δ , *ugeB* Δ] hyphal surface was notable in that its surface
230 appeared fibrillar in the topographic images, hence maximum subunit sizes were not
231 measured. Thus, both UgeA and UgeB appear to be important for wild type hyphal wall surface

232 formation. The [*ugeA* Δ , *ugmA* Δ] strain hyphal wall surface subunits were similar in size to
233 *ugmA* Δ . Taken together, each member of the suite of *Galf* deletion strains produced a
234 distinctive wall phenotype.

235 **Cell wall viscoelasticity and adhesion of wild type and *Galf* biosynthesis gene deletion**
236 **strains**

237 Viscoelasticity is the property describing materials such as hyphal walls, which exhibit
238 both viscous (fluid-like) and elastic mechanical properties. Cell wall spring constants measured
239 by FS (Figure 5A, segment b-c) were used to calculate their viscoelastic modulus for both fixed
240 and live hyphae of AAE1 and the suite of *Galf* gene deletion strains (Table 1). Cell wall
241 viscoelastic moduli for the single deletion strains, *UgeA* Δ and *UgeB* Δ , were significantly lower
242 than that of AAE1 (Table 1). Viscoelastic moduli of *ugmA* Δ and the double deletion strains
243 [*ugeA* Δ , *ugeB* Δ] and [*ugeA* Δ , *ugmA* Δ] were at least an order of magnitude smaller than AAE1
244 (Table 1).

245 Notably, viscoelastic moduli of fixed hyphal walls were typically three-fold higher than
246 that of live ones (Table 1). Hyphal wall viscoelasticity for the suite of *Galf* deletion strains
247 exhibited the same trend for fixed and live hyphae.

248 The Si₃N₄ AFM probes used in this study have hydrophilic surfaces. We used the e-f
249 segment of the FS curve (Figure 5A) to quantify adhesion between *A. nidulans* wall surfaces
250 and the AFM tip during the retraction phase. AAE1 wall surface adhesion to Si₃N₄ is shown in
251 (Table 1). The *ugmA* Δ and [*ugeA* Δ , *ugmA* Δ] hyphae had significantly ($p < 0.05$) stronger
252 adhesion to the hydrophilic tip than wild type hyphae.

253

254 **4. Discussion**

255 Our most notable finding is that perturbing *A. nidulans* cell wall maturation by deleting
256 genes in the *Galf* biosynthesis pathway, has profound effects on wall surface subunit size and
257 packing that are directly associated with cell wall viscoelasticity. This is despite the fact that
258 none of these genes is essential for growth in culture. Previously, we used AFM and FS to
259 show for the first time that growing hyphal tips of a wild type *A. nidulans* strain, A28 (18), had
260 wall surface characteristics that were consistent with long-accepted models of wall deposition
261 and maturation (2, 26) that had yet to be quantitatively tested.

262 El-Ganiny et al. (8, 9) had shown using molecular biology, fluorescence microscopy and
263 TEM that the *ugeA* Δ and *ugmA* Δ deletion strain hyphal morphogenetic defects appeared to be
264 correlated with a lack of immunolocalizable wall *Galf* and to aberrant hyphal wall architecture.
265 Now, we have used high spatial resolution AFM imaging and FS to directly quantify wall
266 defects in this suite of *Galf* biosynthesis gene deletion strains and to compare them to wild
267 type strains.

268

269 ***Galf* is required for wild type *Aspergillus nidulans* hyphal wall formation**

270 This AFM study is the first to make quantitative measurements of cell wall surface
271 subunit features, wall viscoelasticity and adhesive properties of *A. nidulans* strains that had
272 been deleted for enzymes having roles in *Galf* biosynthesis. Strong but circumstantial data in
273 El-Ganiny et al (9) showed that *A. nidulans* strains lacking UgmA had defective hyphal
274 morphogenesis, colony growth, and spore development deficits that correlated with lack of
275 immunodetectable wall *Galf*. Using TEM cross sections, El-Ganiny et al (9) showed that hyphal
276 walls of the *ugmA* Δ strain were more than four times the thickness of AAE1 and had poorly
277 consolidated surfaces suggesting that *Galf* may play a role in wall organization.

278 Previously, we showed using AFM imaging that growing tips of wild type *A. nidulans*
279 had ellipsoidal surface subunits that were larger and more variable in size than the round
280 subunits found 3 μm or further back (Fig 3. in 18). Consistent with the decrease in subunit size
281 and improved organization as a function of maturation, we showed an increase in surface
282 hydrophobicity (Fig. 6D in 18) attributed to decreased exposure of sugar hydroxyl groups.
283 El-Ganiny's study (9) suggested that the *ugmA* Δ strain walls were weaker than wild type since
284 this phenotype was partially remediated by growth on 1 M sucrose.

285 Our present study shows that both *ugeA* Δ and *ugmA* Δ strains had substantially larger
286 surface subunits than AAE1. In contrast, the *ugeB* Δ strains, which had wild type colony
287 phenotype and growth rate, had subunit sizes very similar to AAE1. Thus, it appears that
288 *A. nidulans* surface subunit size is inversely correlated with cell wall maturation in A28 (18) and
289 a suite of deletion mutants in the *Galf* biosynthetic pathway. Our data also show that wall
290 surface organization correlates with wall viscoelastic moduli, and that these data are mirrored
291 by the thickness and surface layer characteristics visualized in hyphal cross sections using
292 TEM.

293 Viscoelastic moduli of fixed and living cell walls had a strong positive correlation,
294 demonstrating the value of comparing fixed strains, thus reducing data collection time. The
295 viscoelastic moduli of fixed hyphal walls were consistently larger, revealing the relationship
296 between chemical cross-linking of the cell wall and its viscoelasticity. The data offer insight into
297 the enzymatic cross-linking of hyphal wall components as an integral step in wall maturation,
298 where cross-linking likely contributes to wall integrity by increasing viscoelasticity.

299 The A4 (28), A28 (18) and AAE1 (current work) are morphological wild type strains. The
300 cell wall viscoelastic modulus of the fixed AEE1 strain was lower than that determined for fixed,
301 rehydrated A4 by Zhao and coworkers (28). Although both studies used the same method to
302 determine cantilever spring constants (5), it is only an estimate and can account for the

303 difference in viscoelastic moduli. The viscoelastic modulus of live AEE1 cell walls (Table 1)
304 was lower than that reported previously for A28 (115 ± 31 MPa; 18). However, since the latter
305 study compared viscoelastic moduli in different regions along single hyphae, cantilevers were
306 not calibrated.

307 We used Zhao's model (18), which assumes the indentation of a contiguous layer (cell
308 wall) surrounding a large cylinder (hyphae; Figure 5B), to calculate cell wall viscoelastic
309 moduli. A plot of the dimensionless unit Eh/k_w versus $(R/h)^{1.5}$ (data not shown) suggests this
310 model fits AEE1, *ugeA* Δ and *ugeB* Δ strains, better than it does the poorly ordered walls of the
311 *ugmA* Δ , [*ugeA* Δ *ugeB* Δ] and [*ugeA* Δ *ugmA* Δ] strains. Differences can at least in part be
312 attributed to the composition and organization of cell wall components (Figure 5B), whereas
313 viscoelastic moduli for *ugmA* Δ , [*ugeA* Δ *ugeB* Δ] and [*ugeA* Δ *ugmA* Δ] strains suggests the AFM
314 tip may penetrate the loosely packed cell wall surface. The Si₃N₄ AFM tips used in this study
315 have tips that are about 5 nm wide (18). The subunits of the *ugmA* Δ and [*ugeA* Δ *ugmA* Δ]
316 strains are 20-fold larger (Table 1), so the AFM tip could possibly pierce an individual subunit.
317 The surface of the [*ugeA* Δ *ugeB* Δ] strain has a fibrillar appearance (Figure 5C), so its
318 interaction with the AFM tip could be unlike the other deletion strains we studied.

319

320 **GalF appears to mediate *Aspergillus nidulans* hyphal wall surface and hyphal adhesion**

321 Lamarre et al (14) suggested that hyphal wall GalF plays a role in *A. fumigatus* hyphal
322 wall surface properties, which they showed qualitatively by the accumulation of material on
323 *Afugm1* Δ hyphal walls using SEM, and by hyphal adhesion to substrates including glass and
324 plastic coverslips, latex beads and epithelial respiratory cells.

325 We quantified the adhesion between the hydrophilic Si₃N₄ AFM tip and walls of living
326 AEE1, *ugmA* Δ and [*ugeA* Δ , *ugmA* Δ] hyphae. The increasing hyphal wall surface disorder in

327 *ugmAΔ* and [*ugeAΔ*, *ugmAΔ*] strains correlates with effects on hyphal wall viscoelasticity and
328 adhesion. The loose packing of hyphal walls surfaces observed by AFM imaging of *Galf*
329 mutants would expose polar groups normally masked during wall maturation, increasing
330 hydrophilic character of the wall surface and resulting in greater adhesion. Consistent with
331 Lamarre et al (14) the *ugmAΔ* and [*ugeAΔ*, *ugmAΔ*] strains tended to adhere to microscope
332 coverslips compared to AAE1 and *ugeBΔ* (data not shown). Adhesion values between the
333 Si₃N₄ tip and *ugmAΔ* and [*ugeAΔ*, *ugmAΔ*] walls were comparable to those previously reported
334 for A28 hyphae at growing tips, where the wall is newly deposited and not yet mature (~ 9 nN,
335 (18)). Thus, surface subunit size, wall viscoelasticity, and wall adhesion to hydrophilic surfaces
336 show consistent trends for wild type and *Galf* gene deletion strains.

337 Schmalhorst et al. (23) provided data to suggest that the *A. fumigatus glfAΔ*
338 (homologous to *A. nidulans ugmA* (9)) strain had attenuated virulence in a murine model for
339 systemic aspergillosis. However, scanning electron microscopy of cross-fractured *glfAΔ* hyphal
340 walls were half the thickness of wild type *A. fumigatus* walls, the opposite trend to our study
341 that deserves further attention.

342 By combining gene deletion characterizations with TEM, AFM, and FS, we have shown
343 that *Galf* is important for *Aspergillus* hyphal wall maturation. However, despite the strong
344 correlation between our results and those of Lamarre et al (14) we are not yet able to
345 determine the likely location(s) of *Galf*-containing molecules in *Aspergillus* walls. Indeed,
346 Latgé's 2010 model (16) discusses these molecules without indicating many details relating to
347 their deployment in the three-dimensional wall architecture.

348 We have shown that perturbing wildtype *Galf* cell wall deposition has substantial effects
349 on the surface ultrastructure and viscoelasticity of the *Aspergillus nidulans* cell wall. *Galf*
350 appears to have crucial and multiple roles in *Aspergillus* hyphal cell wall maturation and

351 integrity. Studies addressing potential roles of mannose in *A. nidulans* wall structure and
352 adhesive properties, and potential roles of Galf in pathogenicity are underway.

353

354 **Acknowledgements**

355 This research was supported by Natural Science and Engineering Research Council of
356 Canada Discovery grants to TESD and SGWK, a Canadian Institutes of Health
357 Research/Regional Partnership Program grant to SGWK, and by an Egyptian Ministry of
358 Higher Education grant to AME. BCP was partially supported by the Department of Chemistry
359 and Biochemistry in the Faculty of Science, University of Regina.

360

361 **References**

- 362 1. **Bar-Peled, M., C. L. Griffith, J. J. Ory, and T. L. Doering.** 2004. Biosynthesis of
363 UDP-GlcA, a key metabolite for capsular polysaccharide synthesis in the pathogenic
364 fungus *Cryptococcus neoformans*. *Biochem. J.* **381**:131-136. doi: 10.1042/BJ20031075.
- 365 2. **Bartnicki-Garcia, S., C. E. Bracker, G. Gierz, R. Lopez-Franco, and H. Lu.** 2000.
366 Mapping the growth of fungal hyphae: orthogonal cell wall expansion during tip growth
367 and the role of turgor. *Biophys. J.* **79**:2382-2390. doi: 10.1016/S0006-3495(00)76483-6.
- 368 3. **Beverley, S. M., K. L. Owens, M. Showalter, C. L. Griffith, T. L. Doering, V. C. Jones,**
369 **and M. R. McNeil.** 2005. Eukaryotic UDP-galactopyranose mutase (*GLF* gene) in
370 microbial and metazoal pathogens. *Eukaryot. Cell.* **4**:1147-1154. doi:
371 10.1128/EC.4.6.1147-1154.2005.
- 372 4. **Cappella, B., and G. Dietler.** 1999. Force-distance curves by atomic force microscopy. *Surf*
373 *Sci Rep.* **34**:5-104.
- 374 5. **Cleveland, J. P., and S. Manne.** 1993. A nondestructive method for determining the spring
375 constant of cantilevers for scanning probe microscopy. *Rev Sci Instrum.* **64**:403-405.
- 376 6. **Damveld, R. A.** 2008. A novel screening method for cell wall mutants in *Aspergillus niger*
377 identifies UDP-galactopyranose mutase as an important protein in fungal cell wall
378 biosynthesis. *Genetics.* **178**:873.
- 379 7. **de Groot, P. W., B. W. Brandt, H. Horiuchi, A. F. Ram, C. G. de Koster, and F. M. Klis.**
380 2009. Comprehensive genomic analysis of cell wall genes in *Aspergillus nidulans*. *Fungal*
381 *Genet. Biol.* **46 Suppl 1**:S72-81.
- 382 8. **El-Ganiny, A. M., I. Sheoran, D. A. Sanders, and S. G. Kaminskyj.** 2010. *Aspergillus*
383 *nidulans* UDP-glucose-4-epimerase UgeA has multiple roles in wall architecture, hyphal
384 morphogenesis, and asexual development. *Fungal Genet. Biol.* **47**:629-635. doi:
385 10.1016/j.fgb.2010.03.002.

- 386 9. **EI-Ganiny, A. M., D. A. R. Sanders, and S. G. W. Kaminskyj.** 2008. *Aspergillus nidulans*
387 UDP-galactopyranose mutase, encoded by *ugmA* plays key roles in colony growth,
388 hyphal morphogenesis, and conidiation. *Fungal Genetics and Biology*. **45**:1533-1542. doi:
389 DOI: 10.1016/j.fgb.2008.09.008.
- 390 10. **Gastebois, A.** 2009. *Aspergillus fumigatus*: cell wall polysaccharides, their biosynthesis
391 and organization. *Future Microbiology*. **4**:583.
- 392 11. **Harris, S. D.** 2009. Morphology and development in *Aspergillus nidulans*: a complex
393 puzzle. *Fungal Genetics and Biology*. **46**:S82.
- 394 12. **Kaminskyj, S. G., and J. E. Hamer.** 1998. hyp loci control cell pattern formation in the
395 vegetative mycelium of *Aspergillus nidulans*. *Genetics*. **148**:669-680.
- 396 13. **Kaminskyj, S. G. W.** 2001. Fundamentals of growth, storage, genetics and microscopy of
397 *Aspergillus nidulans*. *Fungal Genet. Newsl.* 25.
- 398 14. **Lamarre, C., Beau, R., Balloy, V., Fontaine, T., Hoi, J. W. S., Guadagnini, S., Berkova,**
399 **N., Chignard, M., Beauvais, A., and J.-P. Latgé.** 2009. Galactofuranose attenuates
400 cellular adhesion of *Aspergillus fumigatus*. *Cell. Microbiol.* **11**:1612.
- 401 15. **Latgé, J.-P.** 2009. Galactofuranose containing molecules in *Aspergillus fumigatus*. *Med.*
402 *Mycol.* **47 Suppl 1**:S104-9. doi: 10.1080/13693780802258832.
- 403 16. **Latgé, J.-P.** 2010. Tasting the fungal cell wall. *Cell. Microbiol.* **12**:863-872. doi:
404 10.1111/j.1462-5822.2010.01474.x.
- 405 17. **Lesage, G., and H. Bussey.** 2006. Cell wall assembly in *Saccharomyces cerevisiae*.
406 *Microbiol Mol Biol Rev.* **70**:317-343.
- 407 18. **Ma, H., L. A. Snook, S. G. Kaminskyj, and T. E. S. Dahms.** 2005. Surface ultrastructure
408 and elasticity in growing tips and mature regions of *Aspergillus* hyphae describe wall
409 maturation. *Microbiology*. **151**:3679-3688. doi: 10.1099/mic.0.28328-0.

- 410 19. **Ma, H., L. A. Snook, C. Tian, S. G. Kaminskyj, and T. E. S. Dahms.** 2006. Fungal
411 surface remodelling visualized by atomic force microscopy. *Mycol. Res.* **110**:879-886.
412 doi: 10.1016/j.mycres.2006.06.010.
- 413 20. **Momany, M., P. J. Westfall, and G. Abramowsky.** 1999. *Aspergillus nidulans* swo
414 mutants show defects in polarity establishment, polarity maintenance and hyphal
415 morphogenesis. *Genetics.* **151**:557-567.
- 416 21. **Moyrand, F.** 2008. UGE1 and UGE2 regulation of the UDP-glucose/UDP-galactose
417 equilibrium in *Cryptococcus neoformans*. *Eukaryotic Cell.* **7**:2069.
- 418 22. **Perfect, J. R.** 2005. Nuances of new anti-*Aspergillus* antifungals. *Med. Mycol.* **43 Suppl**
419 **1**:S271-6.
- 420 23. **Schmalhorst, P. S., S. Krappmann, W. Vervecken, M. Rohde, M. Muller, G. H. Braus,**
421 **R. Contreras, A. Braun, H. Bakker, and F. H. Routier.** 2008. Contribution of
422 galactofuranose to the virulence of the opportunistic pathogen *Aspergillus fumigatus*.
423 *Eukaryot. Cell.* **7**:1268-1277. doi: 10.1128/EC.00109-08.
- 424 24. **Shi, X., Y. Sha, and S. Kaminskyj.** 2004. *Aspergillus nidulans* hypA regulates
425 morphogenesis through the secretion pathway. *Fungal Genet. Biol.* **41**:75-88.
- 426 25. **Wallis, G. L., F. W. Hemming, and J. F. Peberdy.** 2001. Beta-galactofuranoside
427 glycoconjugates on conidia and conidiophores of *Aspergillus niger*. *FEMS Microbiol. Lett.*
428 **201**:21-27.
- 429 26. **Wessels, J. G.** 1999. Fungi in their own right. *Fungal Genet. Biol.* **27**:134-145. doi:
430 10.1006/fgbi.1999.1125.
- 431 27. **Xu, S., and M. F. Arnsdorf.** 1994. Calibration of the scanning (atomic) force microscope
432 with gold particles. *J. Microsc.* **173**:199-210.

433 28. **Zhao, L., D. Schaefer, H. Xu, S. J. Modi, W. R. LaCourse, and M. R. Marten.** 2005.

434 Elastic properties of the cell wall of *Aspergillus nidulans* studied with atomic force

435 microscopy. *Biotechnol. Prog.* **21**:292-299.

436

437 **Table 1.** Morphological characteristics, maximum dimension of surface subunits, and cell wall
 438 **viscoelastic moduli** of wild type and *Galf* biosynthesis enzyme gene deletion strains.

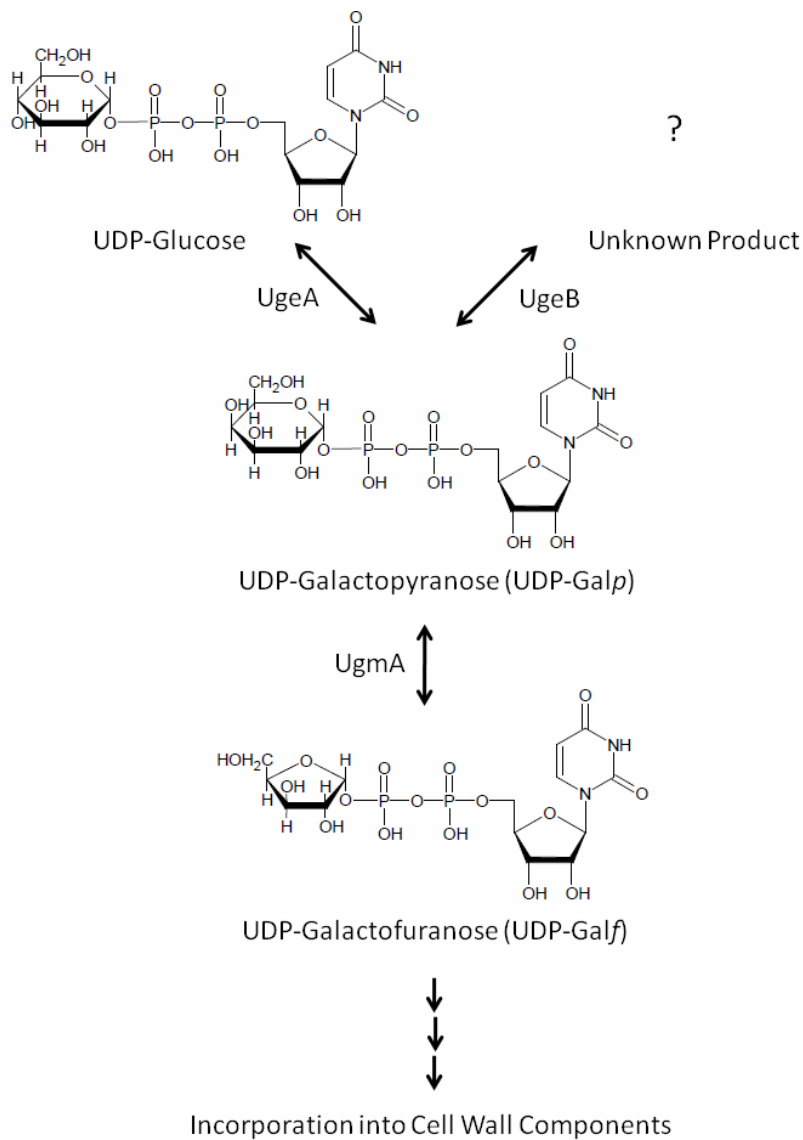
Strain	Hyphal width ^a (μm) \pm SE	Wall thickness ^b (nm) \pm SE	Subunit maximum dimension (nm) \pm SD	Viscoelastic moduli of fixed hyphal wall (MPa) ^c \pm SD	Viscoelastic moduli of live hyphal wall (MPa) ^c \pm SD	Adhesion (nN) \pm SD
Wildtype (AAE1)	2.4 \pm 0.0	54 \pm 2	35 \pm 5	211 \pm 15	82.3 \pm 12.9	5.7 \pm 1.6
<i>ugeA</i> Δ	3.6 \pm 0.1	104 \pm 10	63 \pm 10	99 \pm 48	24.6 \pm 13.7	ND
<i>ugeB</i> Δ	2.5 \pm 0.0	95 \pm 11	39 \pm 8	74 \pm 22	22.5 \pm 8.6	ND
<i>ugeA</i> Δ , <i>ugeB</i> Δ	3.5 \pm 0.1	217 \pm 62	ND ^d	38 \pm 21	9.8 \pm 5.1	ND
<i>ugmA</i> Δ	3.1 \pm 0.1	204 \pm 10	108 \pm 35	14 \pm 2	3.1 \pm 0.4	8.1 \pm 0.3
<i>ugeA</i> Δ , <i>ugmA</i> Δ	3.2 \pm 0.4	162 \pm 8	97 \pm 23	0.05 \pm 0.02	0.03 \pm 0.01	17.3 \pm 3.9

439 ^a There was no significant difference in hyphal width for fixed or live hyphae measured either
 440 by **confocal** microscopy or AFM

441 ^b Measured from TEM hyphal cross-sections. See Materials and Methods section.

442 ^c SD was calculated from errors propagated through equations 1 and 2. See Materials and
 443 Methods section.

444 ^d Not determined. See Results section.



445

446

447

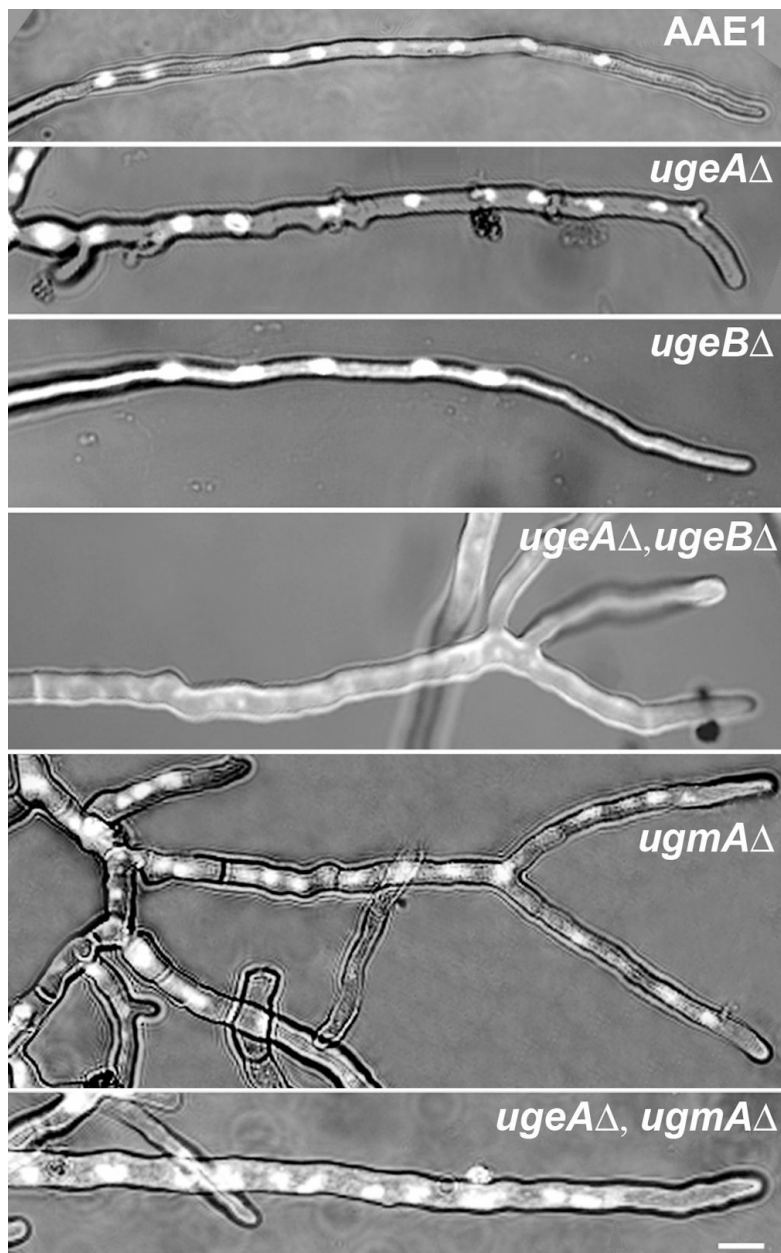
448

449

450

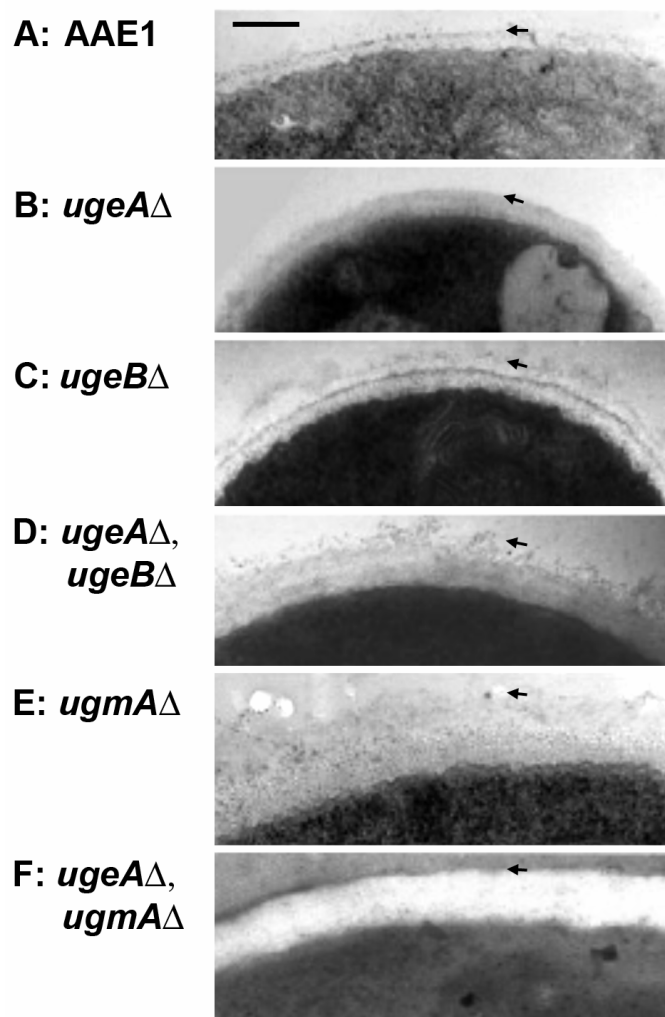
451

Figure 1: Biosynthesis of Galf from UDP-Glucose. UDP-glucose is converted to UDP Galactopyranose by UDP-Glucose 4-epimerase (UgeA). In the reaction shown, UDP galactopyranose is converted to the final product UDP-galactofuranose by UDP galactopyranose mutase (UgmA). These two enzymes are localized in the cytoplasm, and then UDP-galactofuranose is transported to the fungal Golgi equivalent, which is the site of incorporation into other cell wall components.



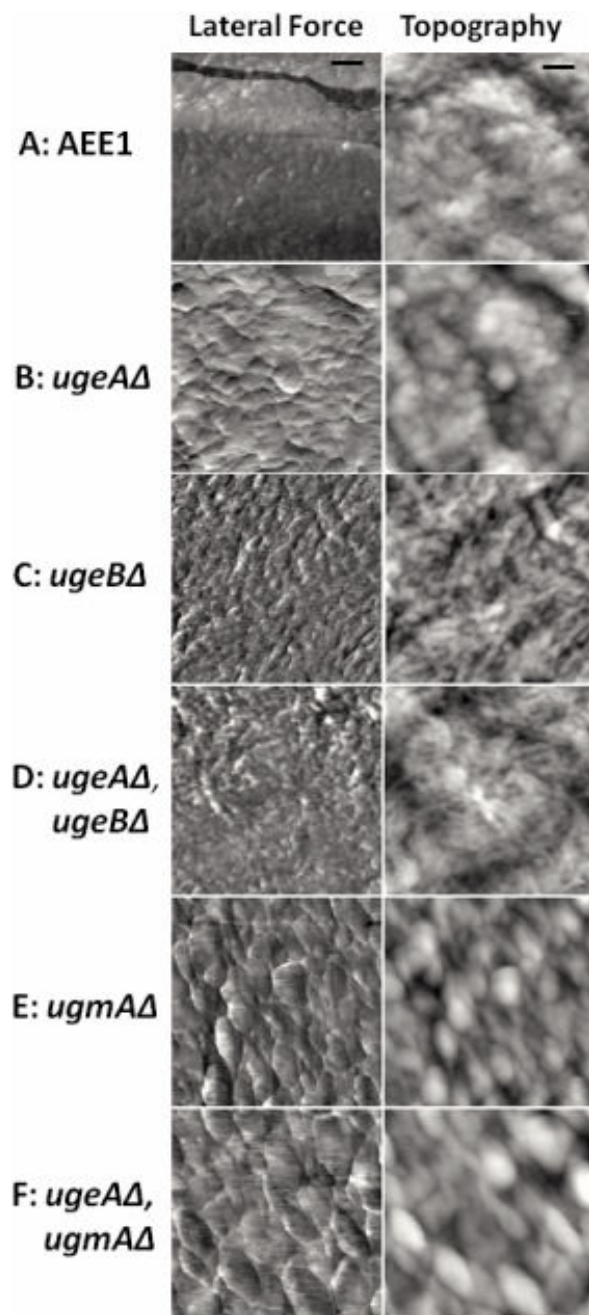
452

453 **Figure 2. Appearance of the wild type and Gal β -biosynthesis deletion strain hyphae used**
454 **in this study.** Strains were grown for 16 h, then fixed and stained with Hoechst 33258 to
455 visualize nuclei. Images are combined fluorescence and transmitted light. Bar = 5 μ m (for
456 all images).



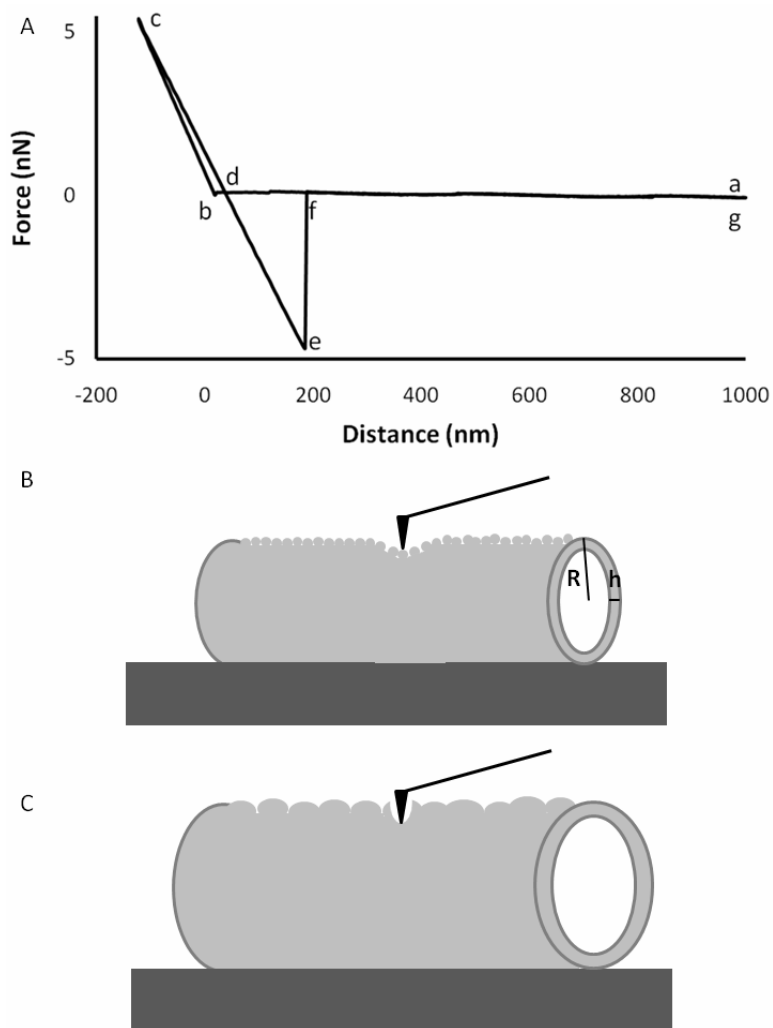
457

458 **Figure 3. Transmission electron micrographs of hyphal wall cross-sections of AAE1 and**459 **GalF-biosynthesis deletion strains used in this study. Bar = 100 nm (in A, wild type**460 **image, for all parts). Impressions regarding the relative hyphal diameter as assessed by**461 **curvature may be misleading, because some hyphal cross sections were not**462 **perpendicular to the hyphal axis. Images have been contrast adjusted to highlight wall**463 **structure; the cytoplasm is dark because wall carbohydrates stain poorly for TEM. [Arrows](#)**464 **[indicate the outer boundaries of cell wall thickness measurements.](#)**



465

466 **Figure 4: Atomic force microscopy images of wild type and GalF-biosynthesis deletion**467 **strains used in this study. Grey scale for lateral force images is ~ 2 nA and for**468 **topography images ranges from 50-70 nm. Bar in A = 200 nm, and is valid for all images.**



469

470 **Figure 5:** A) Representative force curve shows tip approach (a-c) with jump into contact (b)
 471 and tip retraction (c-g). The slope of b-c was used to calculate sample [viscoelastic](#)
 472 [modulus](#) and segment f-e represents tip-sample adhesion. Schematic representation of
 473 the AFM tip (black) interacting with the hyphal surface (grey) of B) AEE1, *ugeA* Δ ,
 474 *ugeB* Δ , in which the entire cell wall is deformed by tip indentation, compared to that of
 475 C) *ugmA* Δ , [*ugeA* Δ ,*ugeB* Δ] and [*ugeA* Δ ,*ugmA* Δ] in which the tip likely deforms the
 476 loosely packed, larger individual subunits or penetrates the space between.